

A SIMPLE FABRICATION OF POLYVINYL PYRROLIDONE (PVP)-COATED Fe_3O_4 NANOPARTICLES TOWARDS IMPROVED CONGO RED DEGRADATION PHOTOCATALYTIC ACTIVITY

P.Rajeswaran^{1,✉}, G. Raja², A. Gilbert Sunderraj³ and P. Kanagambal⁴

¹Department of Chemistry, Vel Tech High Tech Dr.Rangarajan Dr.Sakunthala Engineering College, Chennai-600 062, (Tamil nadu), India

²Department of Chemistry, Paavai Engineering College, Namakkal-637 018, (Tamilnadu), India

³Department of Chemistry, Vinayaka Mission's Kirupananda Variyar Engineering College, Salem-636 308, (Tamil nadu) India

⁴PG and Research Department of Chemistry, Jamal Mohamed College, Tiruchirappalli-620 020, (Tamil nadu) India

✉Corresponding Author: rajesh_chemist@yahoo.com

ABSTRACT

PVP-coated nanoparticles are increasingly being developed for photocatalytic applications. The fabrication of PVP-coated Fe_2O_3 nanoparticles is demonstrated in this work using a novel method. The existence of PVP and Fe_2O_3 phases is identified by powder XRD analysis. SEM, FTIR, and UV techniques were used to examine the morphology and structural examination of the materials. UV-Visible DRS studies reveal optoelectronic transfer and redshifts in PVP-coated composites. Besides, the reduction of average particle size was also identified by SEM and XRD. The potential application of PVP-coated Fe_2O_3 as a photocatalyst was investigated with the use of an aqueous solution of degraded Congo Red dye. Data from photocatalytic research show that Fe_3O_4 -coated PVP (6 wt%) exhibits considerably better photocatalytic activity towards the destruction of CR dyes. The improved photocatalytic activity of the hybrid composite is caused by the combination of phases of PVP and Fe_2O_3 with differing band gaps. Detailed evidence of the photocatalytic activity's mechanism is also provided.

Keywords: PVP, Fe_2O_3 , hybrid nanocomposite, nanospheres, photocatalytic activity, Congo Red,

RASĀYAN J. Chem., Vol. 16, No.1, 2023

INTRODUCTION

Over the last twenty years, environmental concerns have gained international prominence. Globalization is causing significant pollution and eroding the dependability of water supplies, both of which have a direct influence on people's and the general public's health.^{1,2} Textile industry emissions are highly politicized, with a large amount of hazardous and often scarcely biodegradable colorants.^{3,4} So far, the world has generated about 1,000,000 tonnes of various dyes.^{5,6} Azo dyes are a well-known family of coloring chemicals that have a wide range of uses in engineering.⁷ The presence of many azo groups (-N=N-) that interact to produce color differentiates them; when one of these groups is eliminated due to an unanticipated incident, the the-conjugated system is affected, as well as the material's color scheme is lost.^{8,9} The chemical makeup of Congo red dye is shown in Figure.1. It is particularly resistant to damage caused by typical dyeing methods. Due to its enduring presence in the environment, toxicity to aquatic organisms, probable carcinogenic qualities, and capacity to induce skin irritation and allergic reactions in some people, Congo red dye can be hazardous to both the environment and human health. In order to resolve these problems, semiconductors offer a practical solution for the reactive oxygen species that are produced as a result of the photocatalytic action of organic contaminants, such as oxygen in the air and the coloring of visible light.¹⁰

Nanostructured semiconductor materials are an advanced type of photocatalysts because they exhibit unique optical, electrical, and mechanical properties that differ from their bulk counterparts, enabling them to be used in various applications including electronics, optoelectronics, solar cells, sensors, and catalysis. Among the various semiconductor nanomaterials, Fe_3O_4 is promising, inexpensive, and

straightforward to manufacture photocatalyst that also has the ability to separate solids from liquids using an external magnetic field. The removal of Congo red dye utilizing chemically generated Fe_3O_4 nanoparticles as adsorbent was explored by Debnath et al.¹¹ Saad et al., employed the sol-gel process to create two-color dyes, the first one dye is reactive red (RR) and the second dye is malachite green. The dyes nanocomposite with Fe_3O_4 activation for ultrasonic-assisted adsorption.¹² Recent studies report that the photocatalytic performance can be significantly enhanced by constructing a semiconductor/semiconductor hetero junction structure using other materials, this not only enhances the absorption of visible light but also prevents photo-generated electrons and holes from recombining.¹³ For instance, Khashanet al. have successfully produced $\text{Fe}_3\text{O}_4@\text{TiO}_2$ hetero structure nanocomposites, which have an average size ranging from 50-100 nm, markedly different from the size of Fe_3O_4 (2-10 nm) and the thickness of the TiO_2 shell (5 nm) separately.¹⁴ It has been observed from the literature reports that the binding of PVP to gallium ions and complexes can aid in the formation of high-quality $\gamma\text{-Ga}_2\text{O}_3$ nanostructures by reducing initial stage particle formation, crystallization and structural growth of $\gamma\text{-Ga}_2\text{O}_3$ in mild hydrothermal conditions, thus indicating the potential of this method to be applied in the production of $\alpha\text{-Fe}_2\text{O}_3$ nanostructures.¹⁵⁻¹⁶ Surface modification with polymers implanted on magnetic nanoparticles is a novel and appealing approach.¹⁷⁻¹⁸ According to Vadivel et al., PVP coating successfully modifies the CoFe_2O_4 magnetic nanoparticles physical, morphological and magnetic properties..¹⁹ Because PVP polymer is soluble in water, non-hazardous, and frequently utilized in a various field of applications, we employed it as a coating material in this work.²⁰ Compared to other synthesis methods such as solvothermal, and hydrothermal, the precipitation method offers the advantage of producing a small crystalline size, which can be controlled by selecting the appropriate precipitating agent during the reaction.²¹ In order to utilize the advantageous of precipitation method as well as PVP coated iron oxide nanoparticles, In this research, we used the precipitation process to create PVP-coated Fe_3O_4 nanoparticles and we looked at their structural and optical characteristics as a function of polymer concentration, as well as a photocatalytic study to remove Congo red dye from water-soluble solution.

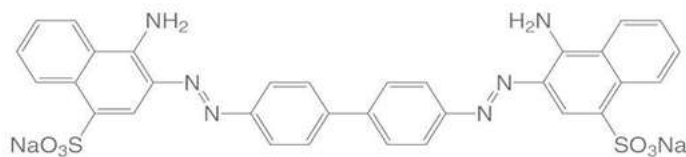


Fig.-1: Congo Red Chemical Structure

EXPERIMENTAL

Material and Methods

The chemicals used in this experiment were all analytically pure and utilized in accordance with the instructions. Ferric chloride hexahydrate ($\text{FeCl}_3 \cdot 6\text{H}_2\text{O}$), Polyvinyl pyridine (PVP), Ferroussulphateheptahydrate ($\text{FeSO}_4 \cdot 7\text{H}_2\text{O}$), (NH_4OH) , congo red dye (CR) and 26% of ammonia were received from merk. The solvent was deionized water. Concentrated water was used to clean all of the glassware. The investigations were conducted entirely with dry equipment.

The creation of PVP-coated iron oxide nanoparticles

Chemical co-precipitation was used to make PVP-coated Fe_3O_4 nanoparticles. In a typical experiment, a 250ml lessened flask was filled with 50ml of 0.01M ferric chloride aqueous solution, 50 ml of 0.033M aqueous solution ferrous sulphate, and 1 g (PVP). To create a standardized solution, the solution mixture was agitated for 30 minutes, additionally 0.25 M ammonia solution was made using 50 mL of deionized water., which was subsequently treated to the solution till the pH achieved 11. On a motorized stirrer, for three hours, the solution was vigorously agitated. at normal temperature. Dark black was created as the solution., which represents the creation of Fe_3O_4 . An everlasting magnet bar was utilized to magnetically filter the supernatant, which was then homogenized in methanol and isolated yet again. To eliminate the excess amine molecules, this process was done four times. Before being calcined for 4 hours at 400 C,

black granular PVP-coated Nanocrystals were dried at room temperature for the complete day.²² Components made from $\text{Fe}_3\text{O}_4/\text{PVP}(2\text{g})$, $\text{Fe}_3\text{O}_4/\text{PVP}(4\text{g})$ and $\text{Fe}_3\text{O}_4/\text{PVP}(6\text{g})$ employing 2,4 and 6 g of PVP, accordingly. The synthesized PVP-coated Fe_3O_4 materials' X-ray diffraction patterns could be seen in the 2 theta range of 10-80 with a step size of 0.025 degrees on an X-ray diffractometer. With the help of a JEOL 6490 LB SEM, radiographs of the compounds were acquired (SEM). At a 3kV working electrical energy, the scanning electron microscopic pictures were obtained. Using Perkin Elmer spectrum two devices, We obtained the substance as-prepared FT-IR spectra. A carry 100 spectrophotometer was employed to collect UV-visible spectra in the 200-800 nm range while operating in absorption mode.

RESULTS AND DISCUSSION

XRD Analysis

XRD analysis was performed on the above-mentioned generated Fe_3O_4 , $\text{Fe}_3\text{O}_4/\text{PVP}(2\%)$, and $\text{Fe}_3\text{O}_4/\text{PVP}(6\%)$ materials to assess phase, crystal arrangement, and purity and it is shown in fig.1. Using the X-ray diffraction peaks in the XRD pattern of such compounds, it is simple to identify the magnetite Fe_3O_4 phase. The materials obtained by calcining a deposit at 400°C for three hours are completely pure Fe_3O_4 , as can be seen from the XRD pattern. Sharp peaks can be seen on the XRD and widened in the diffraction pattern, suggesting the development of Superb $\text{Fe}_3\text{O}_4/\text{PVP}$ materials that are crystalline and compact. The equivalent diffraction peaks to (220) (311) (400) (422) (511) and (440) are nearly comparable to the Fe_3O_4 crystals cubic spinal structure defining peaks. Despite the fact that Scherer's equation is only approximate, it provides an estimate of crystallite size for particles less than 100 nm.²³ The instrumental and sample-dependent effects both contribute to the breadth of diffraction peaks. The average particle size was determined using the XRD peak (311). According to reports, the materials $\text{Fe}_3\text{O}_4/\text{PVP}(0\%)$, $\text{Fe}_3\text{O}_4/\text{PVP}(2\%)$, and $\text{Fe}_3\text{O}_4/\text{PVP}(6\%)$ all had average crystallite sizes of 35, 30, 30 nm.

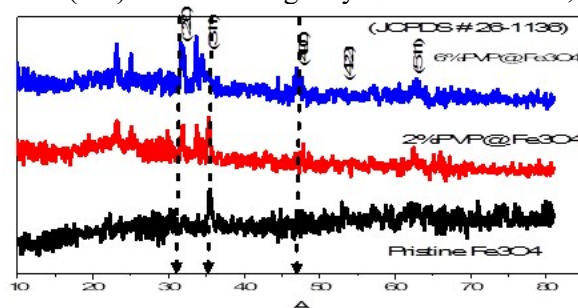


Fig.-2: XRD pattern of a) Fe_3O_4 b) $2\%\text{PVP-Fe}_3\text{O}_4$ c) $6\%\text{PVP-Fe}_3\text{O}_4$

FTIR

Figure-2 illustrates the following FT-IR spectra of nanocrystals decorated with varying amounts of PVP. The stretching frequency of the water molecules' adsorbed -OH band on the surface of PVP-coated Fe_3O_4 nanoparticles causes one peak in the FT-IR spectrum to appear in the $3444\text{--}3401\text{ cm}^{-1}$ range. The peaks that were reached in these samples around 1615 and 1642 cm^{-1} are associated with the intensity of C=O stretching. The magnetite frequencies (at 572 cm^{-1} and 633 cm^{-1} in these samples) represent two vibration bands.²⁴ The IR active mode of vibration has been identified as the source of the single vibrational band at 572 in Fe_3O_4 nanoparticles.²⁵ The C=O absorbance zones shift from 1680 cm^{-1} to 1662 cm^{-1} when PVP concentration rises. The results demonstrate that the carbonyl group in PVP is connected to iron oxide and the reduction in particle size is a result of the manner PVP and Fe_3O_4 interact resulting in the prominence of nanoparticle surfaces. The peak at 1289 cm^{-1} is due to the N-vinyl pyrrolidones C-N stretching vibration. These FT-IR spectra provide substantial evidence that the PVP-coated magnetite nanoparticles originated by C=O interaction.

Scanning Electron Microscopy studies

Fe_3O_4 nanoparticles have a broadly spherical form, according to scanning electron microscopy investigations (fig. 4). According to studies, globular-shaped nanoparticles occur when The interface between Fe_3O_4 magnetic nanoparticles maintained a constant nucleation rate per unit area.^{26,27} Figure 4.a depicts typical SEM micrographs of aggregation of ultrafine particles in the $\text{Fe}_3\text{O}_4/\text{PVP}(0\%)$, $\text{Fe}_3\text{O}_4/\text{PVP}$

(2%), and $\text{Fe}_3\text{O}_4/\text{PVP}$ (6%) samples. The magnetic dipole-dipole interaction between nanoparticles causes agglomeration in these samples.²⁸

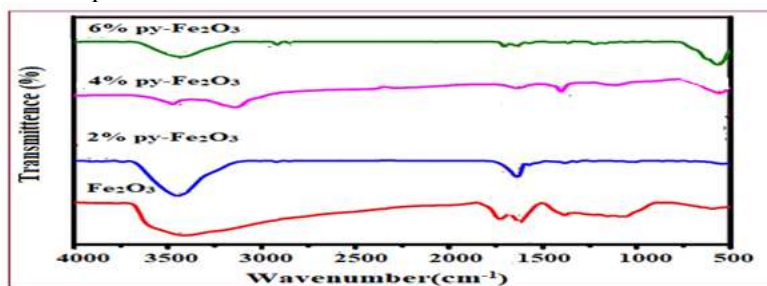


Fig.-3: FT-IR spectra of a) Fe_3O_4 b) 2%PVP- Fe_3O_4 c) 4%PVP- Fe_3O_4 c) 6%PVP- Fe_3O_4

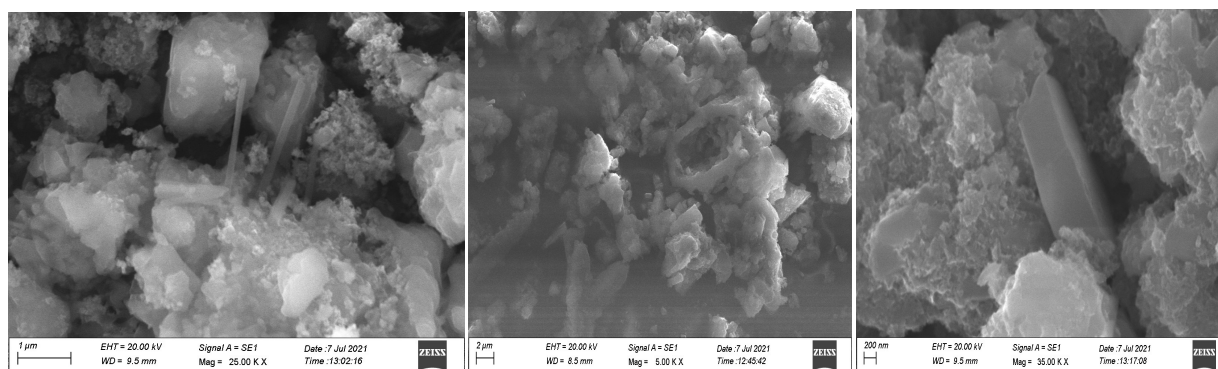


Fig.-4: SEM images of a) Fe_3O_4 b) 2%PVP- Fe_3O_4 c) 6%PVP- Fe_3O_4

UV-Vis DRS analysis

The effectiveness of photo conversion depends on the band gap width and optical absorption capacity. In order to estimate these parameters, UV-Vis DRS was utilized, and the spectra of each sample's optical absorption are shown in Fig. 4a.. Spectra show that all of the substances significantly absorb visible light (410–495 nm). After Polyvinyl Pyrrolidone inclusion, the absorption edge of PVP in Fe_3O_4 is considerably moved towards a higher wavelength (495 nm). The substances' band gap energy is dropping, and the absorption edge of the powdered samples exhibits a clear red shift. The intensity of the band of the samples was determined utilizing the K-M model.^{29,31} The energy band gap values fall from 3.59 to 3.37 eV as PVP concentration rises from 2 to 6 wt%, according to the absorption edge values.

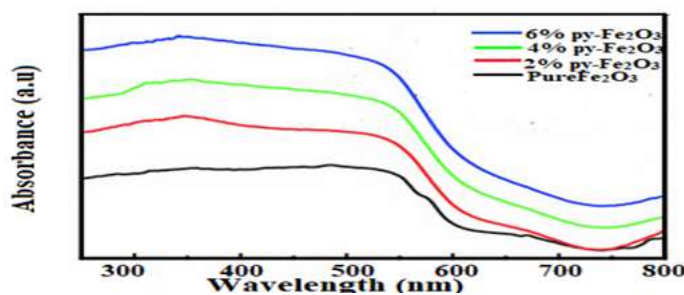


Fig.-5: UV-Spectra of a) Fe_3O_4 b) 2%PVP- Fe_3O_4 c) 4%PVP- Fe_3O_4 c) 6%PVP- Fe_3O_4

Photocatalytic activity measurements

To test the photocatalytic performance of PVP-coated Fe_3O_4 materials, Congo red dye degradation was used. According to photocatalytic analysis, Congo red's adsorption-desorption equilibrium is accomplished in the dark for 30 mins. In the beginning, several irradiations of the photocatalytic activity of a synthetic catalyst for the degradation of CR dye were studied. According to the findings, the reactive dye decolorization is significantly impacted by the number of catalysts used and the duration of the irradiation period. Photocatalytic performance information is shown in Figures-7 and 8. The figure showed that when PVP concentrations increased, the photocatalytic activity of PVP-coated Fe_3O_4 increased. Moreover, observing the respective UV absorption peak of Fig.6, the absorption intensity of

the dye molecule continuously decreases when increasing the irradiation time. The complete vanishing of peak observed only after 120 minutes, suggests the photoactivity of materials and photodegradation increases with increased time. The efficiency of materials to degrade the CR dye was measured by the standard expression $\eta = (1 - C/C_0) \times 100$, C_0 is the level of CR concentration prior to lighting, and C represents the dye concentration following a specific irradiation period. The enhanced photocatalytic performance of the materials was estimated to be 36, 45, and 78% for pristine, 0%, 2% and 6% of Fe_3O_4 samples respectively after 120 minutes. After 120 minutes of UV exposure, Fe_3O_4 samples coated with PVP (6 wt%) showed a tremendous rise in the catalytic efficiency of CR dye. PVP coating (6 wt%) effective responses to the photocatalytic activity, with Congo red dye degradation having the highest decolorization at 78%. This might be explained by the fact that PVP-coated materials have a larger surface area than uncoated ones. This could boost the effectiveness of the electron-hole separation and offer more places for the adsorption of color molecules to take place.³² Moreover, the materials' reusability was tested (Figure 10). This suggests the sway and reusability of the materials. When the sun's light is present, The separation of the photogenerated holes and electrons may be improved by the VB electrons' capacity to transition to the Fe_2O_3 conduction band. More organic compounds can be attached to the surface of the photocatalyst when it has a desired surface area, which is advantageous for photocatalytic activity.

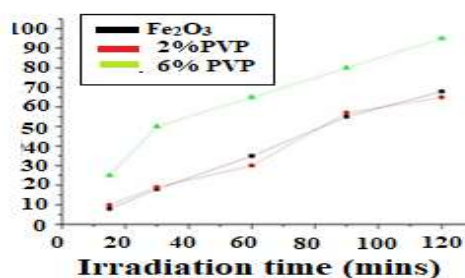


Fig.-7: Photo catalytic degradation efficiency of a) Fe_3O_4 b) 2%PVP- Fe_3O_4 c) 6%PVP- Fe_3O_4

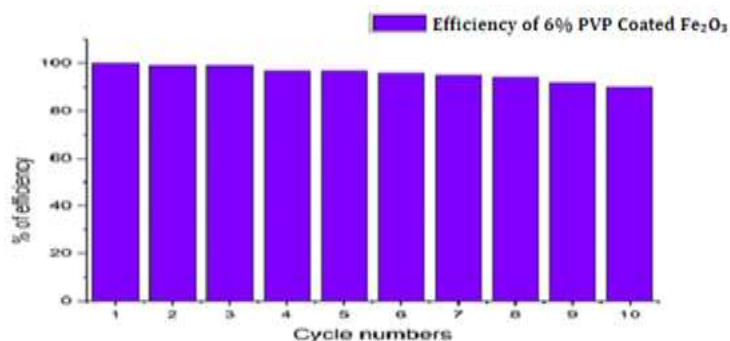


Fig.-8: Cycles of degradation

CONCLUSION

A co-precipitation approach was used to effectively synthesize Fe_3O_4 nanoparticles wrapped in varying quantities of PVP. The Fe_3O_4 /PVP nanoparticles evolved into an inverted spinal structure of crystalline cubes Fe_3O_4 /PVP nanoparticles with high photocatalytic properties due to the huge pore size and surface area. In the above work we checked the photocatalytic activity of Fe_3O_4 /PVP (0%), Fe_3O_4 /PVP (4%) and Fe_3O_4 /PVP (6%) respectively by using a CR as an adsorbent. The highest photocatalytic reaction was found at Fe_3O_4 /PVP (6%) as an adsorbent because it had a huge pore size and surface area compared to others. Congo red's equilibrium took 90 minutes to reach and it is unaffected by the CR dye's original concentration. So it can be said that PVP-coated Fe_3O_4 nanoparticles perform and also adsorbents to absorb the color and consequently, it might be applied to industrial-scale wastewater remediation.

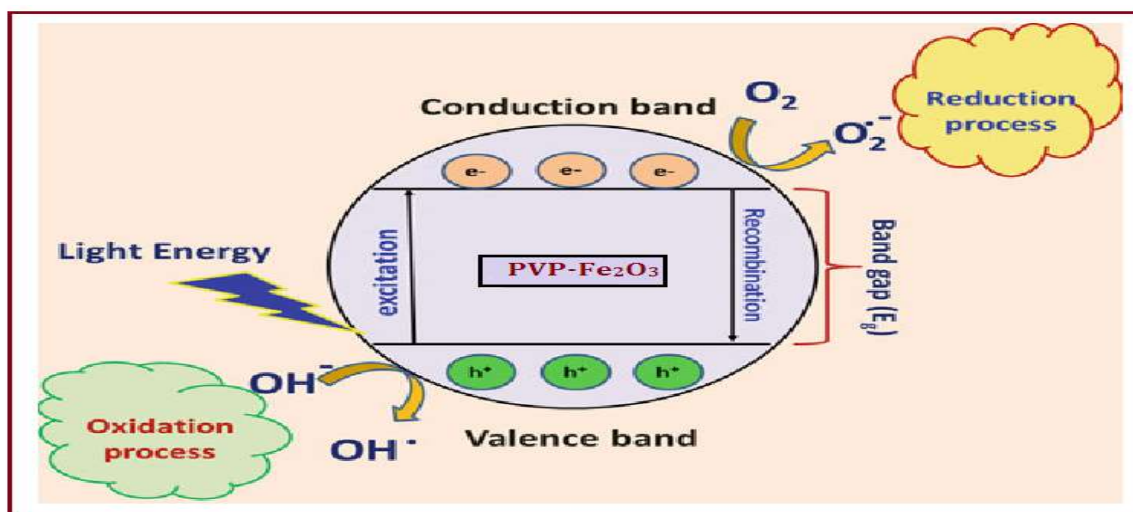


Fig.-9

ACKNOWLEDGEMENTS

To conduct the study, we are grateful for the lab facilities offered by Vel Tech High Tech Dr. Rangarajan Dr. Sakunthala Engineering College, Chennai, 600 062.

CONFLICT OF INTERESTS

The authors state that there is no conflict of interest.

AUTHOR CONTRIBUTIONS

All the authors contributed significantly to this work, took part in its reviewing, editing, and characterizing, and gave their final approval for publication. The author's ORCID IDs which is listed below can be used to confirm their research profile.

P.Rajeswaran  <http://www.orcid.org/0000-00018440-1052>

G.Raja  <http://www.orcid.org/0000-0001-9821-1620>

A.Gilbert Sunderraj  <http://www.orcid.org/0000-0002-4196-5752>

P.Kanagambal  <http://www.orcid.org/0009-0004-1874-0151>

Open Access: This article is distributed under the terms of the Creative Commons Attribution 4.0 International License (<http://creativecommons.org/licenses/by/4.0/>), which permits unrestricted use, distribution, and reproduction in any medium, provided you give appropriate credit to the original author(s) and the source, provide a link to the Creative Commons license, and indicate if changes were made.

REFERENCES

1. S.H.Khan and B.Pathak, *Environmental Nanotechnology Monitoring& Management*, 100290(2020), <https://doi.org/10.1016/j.matpr.2022.11.061>
2. R.Palani, S. Saravanan and R. Kumar, *Rasayan Journal of Chemistry*, **2(3)**, 622(2009)
3. H.Lahmar, M. Benamira, S. Douafer, L. Messaadia, A. Boudjerda and M. Trari, *Chemical Physics Letters*, **742**, 137132(2020), <https://doi.org/10.1016/j.cplett.2020.137132>
4. S.Douafer, H. Lahmar, M. Benamira, G. Rekhila and M. Trari, *Journal of Physics and Chemistry of Solids*, **118**, 62(2018), <https://doi.org/10.1016/j.jpcs.2018.02.053>
5. V.Jegatheesan, B.K. Pramanik, J. Chen, D. Navaratna, C.-Y. Chang and L. Shu, *Bioresource Technology*, **204**, 202(2016),
6. H.Ali, *Water, Air and Soil Pollution*, **213**, 251(2010), <https://doi.org/10.1007/s11270-010-0382-4>
7. S.A.Matar, W. H. Talib and M. A. Al. Damen, *Arabian Journal of Chemistry*, **8(6)**, 850(2015), <https://doi.org/10.1016/j.arabjc.2012.12.039>
8. P. A. Z. Hasibuan, D. Munir, D. Pertiwi, D. Satria, and M. F. Lubis, *Rasayan Journal of Chemistry*, **13**, 4(2020), <http://dx.doi.org/10.31788/RJC.2020.1345625>

9. R.Kumar,N.Swarnalatha and R.Mahesh, *Journal of Molecular Liquid*,**163(2)**,57(2011), <https://doi.org/10.1016/j.molliq.2011.07.010>
10. C.Chen,W.Ma and J.Zhao, *Chemical Society Reviews*, **39**, 4206(2010), <https://doi.org/10.1039/B921692H>
11. P.Bhardwaj, S.Kaushik, P.Gairola and S.P.Gairola, *SN Applied Sciences*,**1**,113(2019), <https://doi.org/10.1007/s42452-018-0115-7>
12. Maleki,Ali,Jamal Rahimi, Oleg M.Demchuk,Agnieszka Z.Wilczewska, and Radomir Jasiński, *Ultrasonics Sonochemistry*, **43**, 262(2018), <https://doi.org/10.1016/j.ultsonch.2017.12.047>
13. J. Hou, H. Cheng, C. Yang, O. Takeda and H. Zhu, *Nano Energy*, **18**, 143-1539(2015), <https://doi.org/10.1016/j.nanoen.2015.09.005>
14. S. Khashan, S. Dagher, N. Tit, A. Alazzam, and I. Obaidat, *Surface and Coatings Technology*, **322**, 92(2027), <https://doi.org/10.1016/j.surfcoat.2017.05.045>
15. Yang, Zun, Ya Qian Wang, Mao MaoRuan, YueTeng, Juan Xia, Jun Yang, Shan Shan Chen, and Fang Wang., *Journal of Materials Chemistry A*, **6(7)**, 2914(2018), <https://doi.org/10.1039/C7TA09913D>
16. Saravanan, K.K.,Siva Karthik, P., Mirtha, P.R.,Balaji, J.,and Rajesh kanna .B, *Journal of Materials Science: Materials in Electronics*, **31**,8825(2020), <https://doi.org/10.1007/s10854-020-03417-4>
17. Fan, Q. L., Neoh, K. G., Kang, E. T., Shuter, B., and Wang, S. C, *Biomaterials*, **28(36)**, 5426(2007), <https://doi.org/10.1016/j.biomaterials.2007.08.039>
18. L. Stanciu, Y.H. Won, M. Ganesana and S. Andreescu, *Sensors*, **9(4)**, 2976(2009), <https://doi.org/10.3390/s90402976>
19. M. Vadivel, R. R. Babu, K. Ramamurthi and M. Arivanandhan, *Nano-Structures & Nano-Objects*, **11**,112(2017),<https://doi.org/10.1016/j.nanoso.2017.08.005>
20. D. Le Garrec, S. Gori, L. Luo, D. Lessard, D. C. Smith, M-A. Yessine, M. Ranger, and J-C. Leroux., *Journal of Controlled Release*, **99(1)**, 83(2004), <https://doi.org/10.1016/j.jconrel.2004.06.018>
21. K. L. Mary, J. V. Manonmoni, A. M. R. Balan, P.S. Karthik and S. P. Malliappan,*Digest Journal of Nanomaterials & Biostructures*, **17(2)**, 634(2022), <https://doi.org/10.15251/DJNB.2022.172.634>
22. K. P. Raj, P. Sivakarthish, A. Uthirakumar and V. Thangaraj, *Journal of Chemical and Pharmaceutical Sciences*,**974**, 2115(2014).
23. G. Hitkari, S. Singh, and G. Pandey, *Nano-Structures & Nano-Objects*, **12**,1(2017), <https://doi.org/10.1016/j.nanoso.2017.08.007>
24. R. M. Cornell, and U. Schwertmann, *Weinheim: WILEY-VCH*, <http://dx.doi.org/10.1002/3527602097>
25. S. H. Shim, and T. S. Duffy, *American Mineralogist*, **87(23)**, 318(2002), <https://doi.org/10.2138/am-2002-2-314>
26. W. Lu, Y. Shen, A. Xie and W. Zhang, *Journal of Magnetism and Magnetic Materials*, **322(13)**, 1828(2010), <https://doi.org/10.1016/j.jmmm.2009.12.035>
27. D. K. Kim, M. Mikhaylova, Y. Zhang and M. Muhammed, *Chemistry of Materials*, **15(8)**,1617(2003), <https://doi.org/10.1021/cm021349j>
28. S. V. Jadhav, D.S.Nikam,V.M. Khot, N. D. Thorat, Manisha R. Phadatare, R. S. Ningthoujam, A. B. Salunkhe, and S. H. Pawar, *New Journal of Chemistry*, **37(10)**, 3121(2013), <https://doi.org/10.1039/C3NJ00554B>
29. Arunprasad, Veeranan, P. Siva Karthik, SelvamThulasi, G. P. Arul, MohdShkir, A. T. Rajamanickam, T.VSumathi and Sonia R. Fredrick, *Journal of Cluster Science*, **33**, 2651(2022), <https://doi.org/10.1007/s10876-021-02183-5>
30. M. Parthibavarman, S. Sathishkumar, S. Prabhakaran, M. Jayashree and R. Boopathi Raja, *Journal of the Iranian Chemical Society*, **15**, 2789(2018), <https://doi.org/10.1007/s13738-018-1466-0>
31. S.Vadivel, G. Rajarajan, *Journal of Material Science;Materials in Electronics.*,**26**, 3155(2015), <https://doi.org/10.1007/s10854-015-2811-z>
32. P. SivaKarthik, V. Thangaraj, S. Kumaresan, and K. Vallalperuman, *Journal of Materials Science: Materials in Electronics*, **28**, 10582(2017), <https://doi.org/10.1007/s10854-017-6832-7>

[RJC-8074/2022]